1. INTRODUCTION

1.0 The Permian-Triassic boundary

The Permian-Triassic boundary is a paleontologically defined transition that separates the Paleozoic and Mesozoic Eras (Erwin, 1993a). The mass extinction associated with the Permian-Triassic boundary makes the boundary one of the most important events in Earth history yet at the present time no Permian-Triassic Global Stratotype Section and Point (GSSP) have been selected. This makes precise definition and identification of the Permian-Triassic boundary difficult. Furthermore biostratigraphic correlation of the Permian-Triassic boundary is not universally accepted. Different workers favour the incoming of different species as indicating the lowermost Triassic. Additionally the correlation of the boundary is complicated by many sections containing a sediment gap at the boundary representing various lengths of time. Erwin (1993a, chapter 2) discusses many of the problems associated with defining the Permian-Triassic boundary and highlights the alternative placements of the boundary proposed on biostratigraphical grounds.

A technique called graphic analysis has been employed to determine which fossils are most suited to define the Permian-Triassic boundary and identify complete sections (Sweet, 1993; Erwin, 1993a). Graphic analysis involves choosing a reference section, then plotting first and last appearances of species in that section against a test section. Assuming that the depositional environments of the sections were similar and the data set is relatively complete for fossil appearances, the plot of the first and last appearances should be a straight line with the slope of the line giving an indication of relative sediment accumulation rates. Periods of non deposition in a section will plot as kinks in the line. This comparison of two sections can then be used to construct a composite section of highest last and lowest first species appearances which can then be used to test new sections and so build up a detailed analysis of faunal time-ranges.

Graphic correlation of the most common biostratigraphical schemes used to define the Permian-Triassic boundary, namely ammonoid and conodont biostratigraphical schemes, has been applied to the traditionally most referenced Permian-Triassic boundary lithological sections (Sweet, 1992). This examination of Guryul Ravine in Kashmir, Zaluch Composite and Salt Range in Pakistan, Shangsi, Sichuan and Meishan in China, Kuh-e-Hambast, Kuh-e-El Bashi and Dorasham II all in Iran, and Nakhichevan in Armenia indicates that conodont-based biostratigraphy is more useful in its ability to recognise complete marine sections across the Permian-Triassic boundary than biostratigraphical schemes based on other fossils.

Along these lines, the first appearance of the conodont *Hindeodus parvus (Isarcicella? parva* of Sweet, 1992*)* has been suggested as the index fossil for the Permian-Triassic boundary (Yin, 1993; Permian Triassic Boundary Working Group (PTBWG), 1993; Paull and Paull, 1994). However, Erwin (1993, fig, 2.17), suggests the incoming of *Neogondollela changxingensis* better marks the Permian-Triassic boundary. In discussing the Permian-Triassic boundary herein, I have accepted the incoming of the conodont *H. parvus* as closely approximating the boundary.

Sweet's (1992) graphic analysis of Permian-Triassic boundary sections indicates sections having latest Permian and earliest Triassic strata. The graphic analysis indicates continuity of section in Dorasham II, Kuh-e-Ali Bashi, Kuh-e-Hambast, Guryal Ravine, Shangsi, and Meishan. Extensive $\delta^{13}C_{CO3}$ ($\delta^{13}C$ of carbonate carbon) studies in most of these sections provide biostratigraphically

calibrated $\delta^{13}C$ profiles that can be compared with $\delta^{13}C$ profiles of sections with weak or no biostratigraphical control, such as facies unsuitable for the preservation of conodonts, in particular nonmarine environments.

Comparison of $\delta^{13}C$ profiles also sheds light on the depositional history. For example, a sharp change in $\delta^{13}C$ values in a section elsewhere known to be gradual suggests the section is condensed or is disconformable (Baud et al., 1989).

1.1 The Permian-Triassic boundary in Australia

The position of the Permian-Triassic boundary in Australian sequences is uncertain. Many Australian Permian-Triassic sedimentary basins are nonmarine and those that are interpreted as marine are dominated by siliciclastic sediments. Carbonate sections that might yield conodonts or a shelly fauna diagnostic of the Permian-Triassic boundary are unknown.

The Permian-Triassic boundary in Eastern Australia was traditionally placed at the boundary between the coal measures and the overlying strata in the Sydney and Bowen Basins (David, 1950). Subsequently, on the basis of correlation of palynomorph assemblages from Eastern Australia with those of Salt Range, Pakistan, Balme (1970) placed the Permian-Triassic boundary at the top of the miospore *Protohaploxypinus microcorpus* Zone (Balme, 1970; Helby et al., 1987).

Briggs (1993a) recognised that Balme's (1979) discovery of an earliest Triassic microflora in East Greenland apparently equivalent to the Tr1a (= *Protohaploxypinus microcorpus*) microflora suggested the Permian-Triassic boundary was in close coincidence with the coal measures/barren measures boundary and the base of the palynological *P. microcorpus* Zone in Eastern Australia. This interpretation reinstated the Permian-Triassic boundary to its traditional place, but was untested. The negative $\delta^{13}C$ excursion about the Permian-Triassic boundary was therefore employed in a test.

The Permian-Triassic boundary in the Salt Range provides a direct link with the Tethyan margin. The negative $\delta^{13}C_{CO3}$ excursion in the Salt Range is poorly defined (Fig. 1.1) but according to Baud et al. (1989) the $\delta^{13}C_{CO3}$ excursion occurs in Unit 4 which contains the palynological *Playfordiaspora crenulata* Zone (Foster, 1982), itself not diagnostic of age. Age-diagnostic fossils are fusulinaceans in the Permian and conodonts in the Triassic. The Kathwai Member coincides with the *H. parvus* Zone (= *I. isarcica* Zone of Sweet, 1992, p. 131) and is therefore earliest Triassic. Dolby and Balme (1976) equate the Kathwai and Mittiwali Members of the Mianwali Formation with the palynological *Kraeuselisporites saeptatus* Zone, which has its type section in the BMR10 (Beagle Ridge) Corehole, Perth Basin, Western Australia. Unit 3 of the the Chhidru Formation is pre-Changhsingian or ?Djulfian (Pakistani Japanese Research Group (PJRG), 1985, table 2) but unit 4 is devoid of marine indicator fossils and the carbonates in this interval have boron values suggesting the influence of fresh water (PJRG, 1985) and hence probable interaction with meteoric waters and diagenetic alteration of the primary marine $\delta^{13}C_{CO3}$ signal. These samples are encircled (Fig. 1.1). The profile of $\delta^{13}C_{CO3}$ in the Salt Range (Baud et al., 1989) without these calcite samples has a negative excursion at the base of the Kathwai Member. My current interpretation of the Salt Range section (Fig. 1.1) places the Permian-Triassic boundary at the top of Unit 4 and differs from Morante, (1993, fig. 2b) that places the Permian-Triassic boundary at the negative excursion in $\delta^{13}C_{CO3}$ at the freshwater-influenced calcite. The *Protohaploxypinus microcorpus* Zone that separates the *P. crenulata Zone* and the *K. saeptatus* Zone is, however, apparently not preserved in the Salt Range section. A critical test of this interpretation of the placement of the Permian-Triassic boundary is the determination of whether the *P. crenulata* Zone is above or below the negative $\delta^{13}C$ excursion elsewhere.

In the type section of the *P. crenulata* Zone in Denison NS20 corehole (Foster, 1982, fig. 5) in the Bowen Basin, Eastern Australia, the *P. crenulata* Zone occupies the uppermost 7 m of the Rangal Coal Measures between the Upper Stage 5 palynological zone and *P. microcorpus* Zone. Foster (1982), interpreted this interval as time equivalent to Unit 4 Salt Range. In the Denison NS20 Corehole, $\delta^{13}C_{org}$ ($\delta^{13}C$ of organic carbon) stratigraphy around the interval of the *P. crenulata* Zone was therefore identified as critical for resolving the age of Unit 4 of the Chhidru Formation, Salt Range and the consequent identification of the Permian-Triassic boundary in Eastern Australia.

Figure. 1.1 Nammal Gorge, Salt Range, Pakistan, showing formations, zones, and $\delta^{13}C_{CO3}$. Permian part of the section, including lithological log and formations from PJRG (1985, fig. 6, columns B and C). Ages of the Permian part of the section from fusulinaceans (PJRG, 1985, table 2). Triassic part of the section from Haq et al. (1988, fig. 13), including formations, sequences (labelled W-Z), and conodont zones (labelled a-j), from *H. parvus* (a) to *N. timorensis* (j), and stages (Matsuda, 1985, fig.1; Haq et al. 1988). The *P. crenulata* Zone (CREN) is in Unit 4 of the Chhidru Formation (Foster, 1982, fig.6). The encircled $\delta^{13}C_{CO3}$ values are those suspected to have been diagenetically altered to more negative values. Their interpreted primary values are probably more positive values as indicated by the arrow.

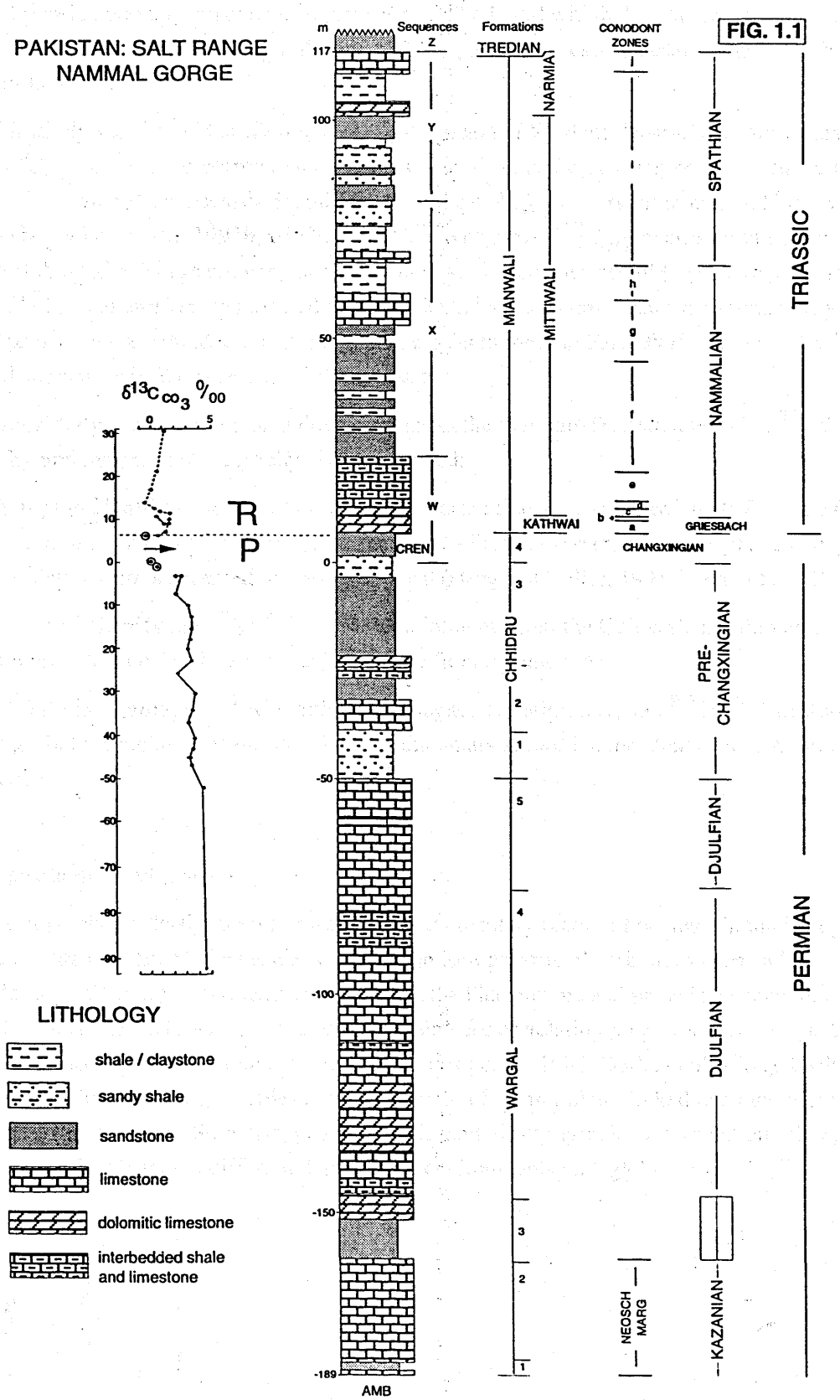
PAKISTAN: SALT RANGE
NAMMAL GORGE
FIG. 1.1
m
Sequences
Formations
CONODONT ZONES
TREDIAN
NARMIA
MIANWALI
MITTIWALI
KATHWAI
CREN
Z
Y
X
W
117
100
50
0
-50
-100
-150
-189
AMB
δ13Cco3 %00
0
5
30
20
10
0
10
20
30
40
-50
-60
-70
-80
-90
R
P
LITHOLOGY
shale / claystone
sandy shale
sandstone
limestone
dolomitic limestone
interbedded shale and limestone
CHHIDRU
WARGAL
4
3
2
1
5
4
3
2
1
a
b
c
d
e
f
g
h
i
CHANGXINGIAN
GRIESBACH
NEOSCH MARG
SPATHIAN
NAMMALIAN
PRE-CHANGXINGIAN
DJULFIAN
DJULFIAN
KAZANIAN
TRIASSIC
PERMIAN

1.2 Project development

The initial aim was to establish whether the $\delta^{13}C_{CO3}$ negative excursion found in marine Tethyan Permian-Triassic boundary carbonate sequences could be found within Australian siliciclastic sediments using $\delta^{13}C_{org}$. The use of $\delta^{13}C_{org}$ rather than $\delta^{13}C_{CO3}$ was necessary because the Gondwana facies effectively lacks carbonate.

I initially sought to identify the $\delta^{13}C_{org}$ excursion in Western Australian sedimentary basins via marine $\delta^{13}C_{org}$ and then to correlate the Permian-Triassic boundary by palynology to Eastern and Central Australia. Following the successful identification of the $\delta^{13}C_{org}$ excursion in marine Northwestern Australia (Morante, 1993a; 1993b; 1993c) I sought the negative $\delta^{13}C_{org}$ excursion in nonmarine Eastern and Central Australia. These studies, the first of their kind, were successful (against expectation) in that the negative $\delta^{13}C_{org}$ excursion was located in West, Central and Eastern Australian sedimentary basins. The $\delta^{13}C_{org}$ profiles were extended down the geologic column into the Early Permian in biostratigraphically controlled sequences in Western and Eastern Australia.

Subsidiary projects were then developed about the Permian-Triassic interval in $^{87}Sr/^{86}Sr$ stratigraphy and magnetic stratigraphy. These included:

1) An attempt to identify the end of the Kiaman Reversed Superchron in sediments from the Cooper Basin and define the relationship of the $\delta^{13}C_{org}$ excursion (= Permian-Triassic boundary) to a change in magnetic polarity from a reversed to normal interval (Haag and Heller, 1991; Heller et al., 1995).

2) An attempt to identify the $^{87}Sr/^{86}Sr$ seawater minimum about the Ochoan/Guadalupian boundary (Denison et al., 1994) using low-magnesium calcite from brachiopods.

The three techniques, $\delta^{13}C$ stratigraphy, magnetic stratigraphy, and $^{87}Sr/^{86}Sr$ stratigraphy, represent globally synchronous markers in the sedimentary record independent of biostratigraphical correlation.

1.3 Isotope chemostratigraphy

Isotope chemostratigraphy is based on the sedimentary record of changes in the isotope ratio of certain elements with time. The secular variations in isotope pairs of carbon, oxygen, sulfur and strontium in seawater are relatively well documented through the Phanerozoic and provide a geochemical correlation tool (Fig. 1.2). Attempts to use these secular variations for correlation purposes have been mooted since the 1970's (for example, Veizer and Hoefs, 1976; Veizer et al., 1980; Burke et al, 1982). Carbon isotope chemostratigraphy potentially enables the development of a chronology linked to a numerical time scale through integration with radiometric, paleomagnetic, and biostratigraphical correlation schemes, and can be used to correlate between different depositional environments on a global scale.

In the case of carbon or oxygen the δ method of reporting is used where

$$\delta = \frac{R_{sample} - R_{reference}}{R_{reference}} \times 1000$$

in which R is the ratio $^{13}C/^{12}C$ for $\delta^{13}C$ or $^{18}O/^{16}O$ for $\delta^{18}O$ and is expressed as a permil (‰) deviation from the standard. In this study the standard referred to for $\delta^{13}C$ and $\delta^{18}O$ is the PDB standard (Urey et al., 1951; Craig, 1957). Tn the case of Sr, the ratio of $^{87}Sr/^{86}Sr$ is compared directly.

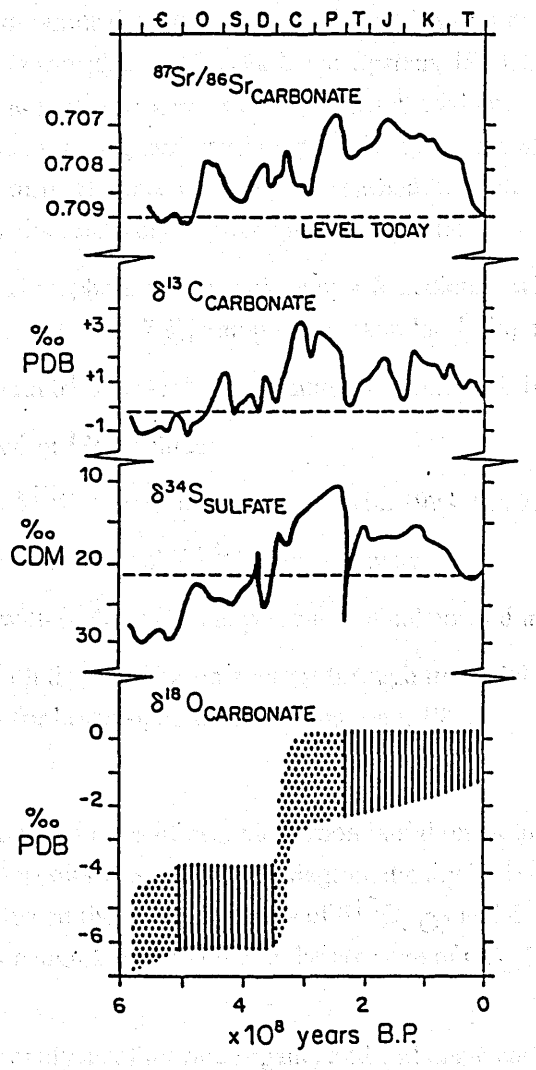

Figure 1.2 Secular isotopic age curves for seawater as derived from strontium isotopes in carbonates and fossil apatites, carbon from carbonates, sulfur from evaporite sulfates, oxygen from carbonates. After Veizer et al. (1986).

Elements useful for isotope chemostratigraphy include carbon from carbonates ($\delta^{13}C_{CO3}$), or organic sources ($\delta^{13}C_{org}$), sulfur from sulfates or pyrite, and strontium ($^{87}Sr/^{86}Sr$) from marine carbonate. Except for $\delta^{13}C_{org}$ their potential as correlation tools is usually restricted to marine sediments. The isotopic composition of the elements in the oceanic reservoir is generally homogeneous because their residence times are greater than the mixing times for the oceanic water mass (Broecker and Peng, 1982). This is not the case for the bulk terrestrial reservoir of these elements except carbon because of the existence of substantial discrete sub-reservoirs or because local environmental factors affect isotopic compositions on a time scale less than that for mixing between the sub-reservoirs. For the oceanic and continental reservoirs of carbon, however, there is an interactive link ensuring equilibration through atmospheric carbon dioxide, which on a geological time scale is rapid being of the order of <50 years for exchange between the ocean mixed layer and the atmosphere and <5000 years for marine carbon turnover in the oceans (Koch et al., 1992). Because of this interaction, decoupling of the oceanic and continental carbon reservoirs is limited to geologically brief time-spans.

The two stable isotopes of carbon, ^{13}C and ^{12}C, are distributed differently between organic (reduced) and inorganic (oxidised) compounds primarily because of the preferential partitioning of ^{12}C into reduced carbon compounds during photosynthesis which results in a fractionation of approximately –20‰ from the $\delta^{13}C$ of atmospheric CO_2 (Park and Epstein, 1960; Schidlowski, 1988). A change in the $\delta^{13}C_{org}$ of terrestrial and marine organic matter, which is predominantly of plant origin therefore reflects a change in the $^{13}C/^{12}C$ of atmospheric carbon dioxide at the time of photosynthetic reduction by plants (O'Leary, 1988), and in turn reflects a change in the carbon flux rates between oxidised and reduced reservoirs. Those reservoirs relatively depleted in ^{13}C include:

- the organisms of the biosphere and organic matter in sediment with $\delta^{13}C = -25‰$ on average during the Permian (Erwin, 1993, fig. 7.8), and probably similar during the earlier Paleozoic, and
- clathrate methane with $\delta^{13}C = -65‰$ on average (Erwin, 1993, fig. 7.8).

Those relatively enriched in ^{13}C include:

- Mantle carbon with $\delta^{13}C = -5‰$ on average (Erwin, 1993, fig. 7.8).
- CO_2 dissolved in the oceans with $\delta^{13}C = 0‰$ on average.
- Atmospheric CO_2 with $\delta^{13}C = -7‰$ at present, but unknown during the Permian, and
- carbonate carbon with $\delta^{13}C = 0‰$ on average through time (Schidlowski, 1983) but generally >4‰ during the Permian for brachiopod calcite (Grossman, 1994).

The idea that lowered rates of organic carbon burial result in a parallel decrease in $\delta^{13}C_{CO3}$ and $\delta^{13}C_{org}$ in surficial reservoirs was developed diagramatically by Hayes and reported in Knoll (1991) (Fig. 1.3). The difference between the primary values of $\delta^{13}C_{CO3}$ and $\delta^{13}C_{org}$ (referred to as Δ) remains constant unless there is a significant change in the pressure of CO_2 (Popp et al., 1989; Magaritz et al., 1992).

Where tandem analysis of marine organic and carbonate carbon can be made the relationship between $\delta^{13}C_{CO3}$ and $\delta^{13}C_{org}$ enables determination of whether samples represent a true record lacking the effects of diagenesis or biodegradation. Significant divergence of either $\delta^{13}C_{CO3}$ or $\delta^{13}C_{org}$ resulting in unusually small or large Δ values indicates a high probability of diagenetic re-equilibration. According to Knoll et al. (1986), Δ values indicating the preservation of a primary signal are 28.5‰ ±2‰.

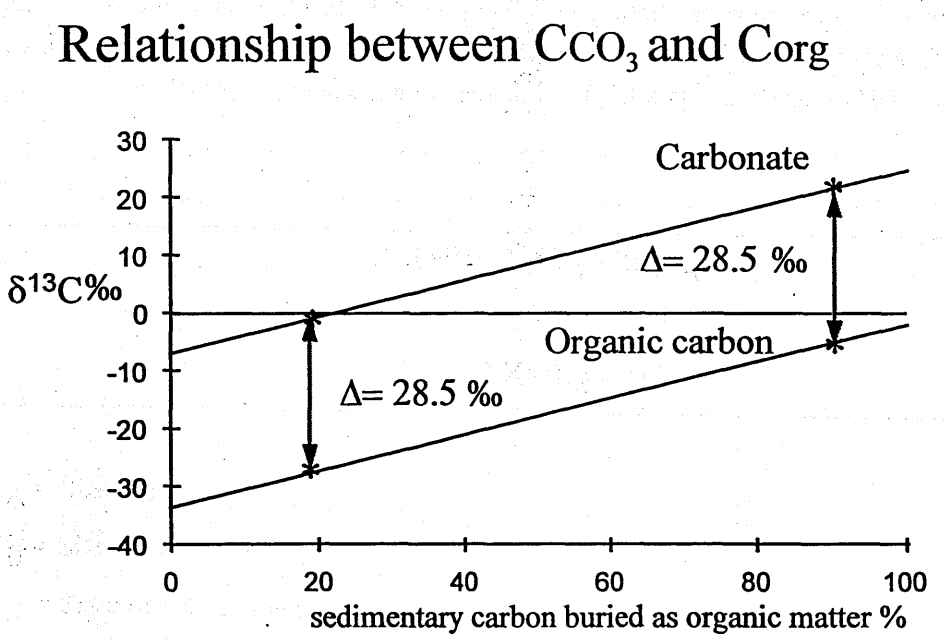

Figure 1.3 Variation of $\delta^{13}C_{CO3}$ and $\delta^{13}C_{org}$ in parallel as a function of variation in the % of carbon buried as organic carbon in sediments. After Knoll (1991).

The $^{87}Sr/^{86}Sr$ seawater curve is useful as a stratigraphic tool because strontium is homogeneous in well-mixed seawater at any given moment (Jones et al., 1994). This is largely because the residence time of strontium in the oceanic reservoir is of the order of 4 million years which is three orders of magnitude longer than the mixing time for the world ocean (Veizer, 1989). The $^{87}Sr/^{86}Sr$ has undergone secular variation as a result of the relative fluxes of radiogenic strontium from continental weathering ($^{87}Sr/^{86}Sr \geq 0.71$) and relatively nonradiogenic strontium injected into the oceans by mid-oceanic ridge hydrothermal activity ($^{87}Sr/^{86}Sr \cong 0.703$). Variations in the $^{87}Sr/^{86}Sr$ reflect the relative waxing and waning of these two sources (Jones et al., 1994). One of the most dramatic of these Phanerozoic secular variations in $^{87}Sr/^{86}Sr$ occurs during the Permian (Fig. 1.2).

1.4 Negative excursions in global $\delta^{13}C_{CO3}$ and $\delta^{13}C_{org}$

The ocean currently contains around 65 times more carbon (as HCO_3^-, CO_3^{2-} and CO_2) than the atmosphere (Siegenthaler and Sarmiento, 1993). Atmospheric CO_2 re-equilibrates with the ocean's mixed layer (approximately the top 1000 m) in a few to tens of years (Broecker and Peng, 1982) hence any change in the mixed layer of the world ocean of the day must be reflected in the CO_2 of the atmospheric environment. Any atmospheric CO_2 variation lasting a significant time ($> 10^2$ years) is therefore associated with a fundamental change in ocean geochemistry. Assuming that the global surficial carbon mass has remained constant within narrow limits, then any significant alteration in the $\delta^{13}C_{CO3}$ and

$\delta^{13}C_{org}$, as about the Permian-Triassic boundary, indicates a fundamental change in the carbon cycle. Tracking of that negative $\delta^{13}C$ excursion across environments therefore provides a stratigraphic datum.

Negative excursions in global $\delta^{13}C_{CO3}$ and $\delta^{13}C_{org}$ reflect an increased flux of carbon from ^{13}C-depleted to ^{13}C-enriched reservoirs. The amount of carbon required to produce a given excursion in $\delta^{13}C_{CO3}$ can be calculated using the equation developed by Spitzy and Degens (1985).

$$N_B = N_A * \frac{(1+R_B) \times (R_A - R_M)}{(1+R_A) \times (R_M - R_B)}$$

Where

N_A = Size of reservoir A

N_B = Size of reservoir B

R_A = Ratio of isotopes in reservoir A

R_B = Ratio of isotopes in reservoir B

R_M = Ratio of isotopes in mixed reservoirs A+B

The ratio of the isotopes of carbon for any $\delta^{13}C$ value can be calculated by solving the equation for δ assuming the $^{13}C/^{12}C$ ratio determined by Craig (1957) for PDB.

Erwin (1993) performed the calculations for a $\delta^{13}C_{CO3}$ excursion from 3 to -1‰, the excursion in $\delta^{13}C_{CO3}$ about the Permian-Triassic boundary in whole rock carbonates (Grossman, 1994). From an estimated 40,000 GT of dissolved inorganic carbon (DIC) in the Permian world ocean, the 4‰ excursion is calculated to have required a transfer of approximately 8-10 global biomasses (total amount of carbon in all living organisms) from the reduced to the oxidised global reservoirs, or 40 000 GT of mantle carbon (which is about 60 times the present mass of atmospheric CO_2) with $\delta^{13}C$ of -5‰ to have been erupted from volcanoes.

These simple calculations suggest that a loss of biomass or a large volcanic eruption of CO_2 could not directly cause the observed $\delta^{13}C_{CO3}$ isotopic excursion (Erwin, 1993, p. 202; see also Gruszczynski et al., 1989).

1.5 $\delta^{13}C_{CO3}$ about the Permian-Triassic boundary

The Late Permian/Early Triassic is of particular interest for a $\delta^{13}C$ investigation because it is the time of the largest extinction event during the Phanerozoic (Sepkoski, 1989; Erwin, 1993; 1994; Stanley, 1994; Benton, 1995). The Permian-Triassic boundary is defined by a decrease in biodiversity in marine sediments, and in Tethyan margin sections and South China, it is accompanied by a dramatic reduction in $\delta^{13}C_{CO3}$ (Baud et al., 1989; Holser et al., 1989; Chen et al., 1991; Xu and Yan, 1993).

A synopsis of the Permian-Triassic $\delta^{13}C_{CO3}$ stratigraphy in China, Austria, and Tethys is shown in Fig. 1.4, (Grossman, 1994). These section locations are shown on Fig. 1.5.

$\delta^{13}C$ profiles about the Permian-Triassic boundary from southern Gondwanaland have been lacking until this study because the main emphasis has been on studying the predominantly carbonate

marine sections on the Cimmerian Paleotethyan margin. Grossman (1994) suggested the probable reason most studies have concentrated on whole rock carbonate analysis is the ease of laboratory preparation required. The locations of the Australian sections from this $\delta^{13}C$ study are also shown on Fig. 1.5.

The negative $\delta^{13}C$ excursion at the Permian-Triassic boundary in carbonate sections ranges from 3 to 11‰ (Fig. 1.4). The negative $\delta^{13}C_{CO3}$ excursion in whole rock carbonates is commonly around 3‰ in Tethyan sections (Baud et al., 1989; Grossman, 1994), is up to 11‰ in Chinese sections (Chen et al., 1991; Xu and Yan, 1993), and is about 7‰ in Tibet (Geldsetzer and Wang, 1994). The larger $\delta^{13}C_{CO3}$ excursions have been interpreted as due to diagenesis (Grossman, 1994) because a $\delta^{13}C$ excursion much larger than 3‰ is too difficult to explain by "conventional mechanisms" such as oxidation of buried organic matter or reduction in biomass. A $\delta^{13}C_{CO3}$ excursion of 10‰ requires a flux of as much as 33 000 GT of organic carbon to the oxidised realm (Gruszczynski et al., 1989; Spitzy and Degens, 1985). This amounts to approximately 10 times the carbon contained in the surface ocean, land biota, soil and detritus at the present time (Siegenthaler and Sarmiento, 1993). Such a huge transfer of organic carbon to an oxidised carbon reservoir at the Permian-Triassic boundary is difficult to explain but provides insight into the events about the Permian-Triassic boundary.

$\delta^{13}C_{CO3}$ excursion profiles about the Permian-Triassic boundary fall into two categories: sharp (Meishan Section D, Xu and Yan, 1993) (Fig. 1.6), or gradual (Gartnerkofel Core, Holser et al., 1989) (Fig. 1.7). Baud et al., (1989) concluded that a sharp excursion in $\delta^{13}C_{CO3}$ indicates an hiatus. A sharp $\delta^{13}C$ excursion could however be produced by 1) a rapid change in $\delta^{13}C$ values in a complete section, 2) a break in sedimentation during which time a gradual $\delta^{13}C$ excursion occurred or 3) a condensed section resulting from slow sediment accumulation rates (Erwin, 1993). A gradual $\delta^{13}C_{CO3}$ excursion could be produced by 1) a gradual excursion in $\delta^{13}C_{CO3}$ values, 2) an extremely rapid rate of sedimentation leading to a dilated section or 3) a mixture of carbon with more positive $\delta^{13}C$ values from older sediments being recycled into sediments with carbon having more negative $\delta^{13}C$ values. This would lead to the recycled carbon eventually being totally replaced by more ^{13}C depleted carbon. How this mechanism might work in a limestone section is less clear than how it would work in a siliciclastic section. It is difficult to perceive how a reef could be constructed of reworked and primary limestones and develop the well-mixed profile such as that of the Gartnerkofel Core-1 (Holser et al., 1989; 1991).

Most $\delta^{13}C_{CO3}$ profile excursions about the Permian-Triassic boundary are gradual rather than sharp. Those that are sharp with the exception of Meishan Section D are thought to contain an hiatus at the Permian-Triassic boundary (Baud et al., 1989).

To facilitate comparison of the isotopic profiles on an equal-interval scale, I have calibrated selected biostratigraphical zones in Ma according to the scheme elaborated in Chapter 6. The numerical ages of parts of this and following profiles are shown in bold and will be employed making comparisons on a common numerical scale in Chapter 6.

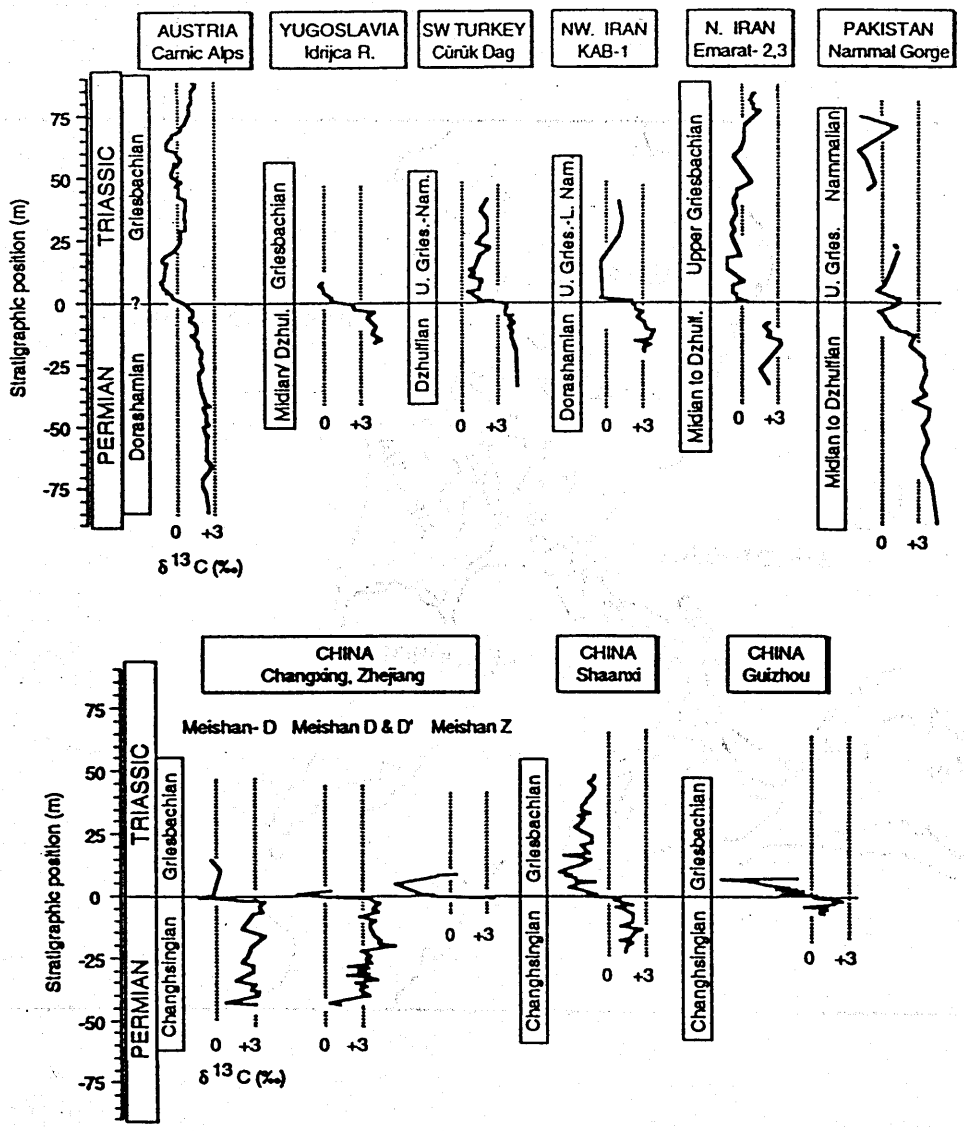

Figure 1.4 $\delta^{13}C_{CO3}$ profiles from Austria, Yugoslavia, southwestern Turkey, northwestern Iran, northern Iran, Pakistan, and China (Zhejaing, Shangsi and Guizhou) about the Permian-Triassic datum (from Grossman, 1994; fig.10). Sections are located on Fig.1.5. No attempt has been made to correlate other than at the paleontologically determined Permian-Triassic boundary.

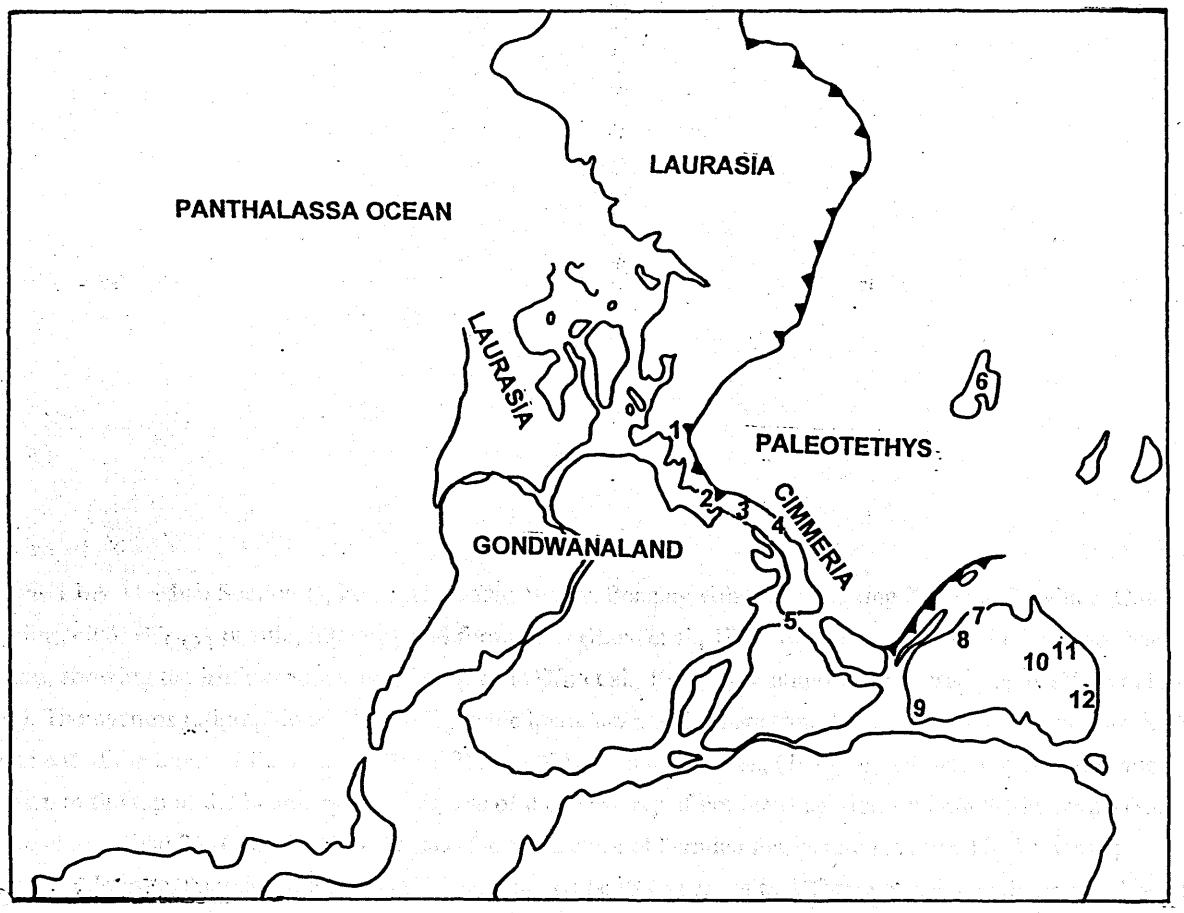

Figure 1.5 Locations of sections shown on Fig.1.4: 1. Gartnerkofel, Carnic Alps and Indrijica River, Southern Alps, 2. Cürük Dag, Turkey, 3. Kuh- e- Ali-Bashi, Northwestern Iran, 4. Emarat-2, 3, Northern Iran, 5. Nammal Gorge, Pakistan, 6. Meishan Section D, Zhejiang, Shangsi, and Guizhou, China. Locations of carbonate sections on a Pangea reconstruction map base after Baud et al. (1989). With the exception of the Salt Range and Chinese sections all carbonate sections are on the Paleotethyan margin of the Cimmerian Arc. Numbers 7 to 12 show the locations where the $\delta^{13}C_{org}$ record has been studied through the Late Permian and Early Triassic in this study: 7. Bonaparte Basin, 8. Canning Basin, 9. Perth Basin, 10. Cooper Basin, 11. Bowen Basin, and 12. Sydney Basin.

Figure. 1.6A Meishan Section D, Zhongxin Dadui quarry, Boaqing village, Changxing Zheijang Province, China, showing the $\delta^{13}C_{CO3}$ profile, lithology and formations (Baud et al., 1989, fig. 14), and **B** detail of the Meishan Section, showing the iridium anomaly, $\delta^{13}C$ profile (Xu et al., 1993), formations and biostratigraphy (Yin et al., 1993). The eventostratigraphic and biostratigraphic boundary positions are from Wang (1995). I have ammended the placement of the topmost Permian and basal Triassic from that of Xu et al., (1993) as follows: Topmost definite Permian to the top of the boundary clay because of the discovery of Permian conodonts within the Permian-Triassic "white clay"(= bed 26) (Yin, 1993, p. 22) and the persistance of Permian fossils into the mixed bed 1 above; lowermost definite Triassic from midway through mixed bed 2 (= base of bed 27c) coinciding with the *Hindeodus parvus* Zone (Yin, 1993, p. 22; Wang, 1995). The asterisk marks the SHRIMP date (251.2 ± 3.4 Ma) determined on zircons from the boundary clay rock (Claoué-Long et al., 1991). To facilitate comparison of the isotopic profiles on an equal -interval scale, I have calibrated selected biostratigraphical zones in Ma according to the scheme elaborated in Chapter 6. The numerical ages of parts of this and following profiles are shown in bold and will be employed making comparisons on a common numerical scale in Chapter 6. The timescale is determined by calibrating the base Dorashamian (= Changsingian) at 253 Ma, Permian-Triassic boundary at 250 Ma, Griesbachian top at 248.7 Ma, and Nammalian top at 247.4 Ma. These procedures are followed for all profiles following where biostratigraphical control is sufficiently well developed to allow an estimate of a numerical age. The $\delta^{13}C$ profiles are subdivided into segments A-D as outlined in Chapter 1.8.

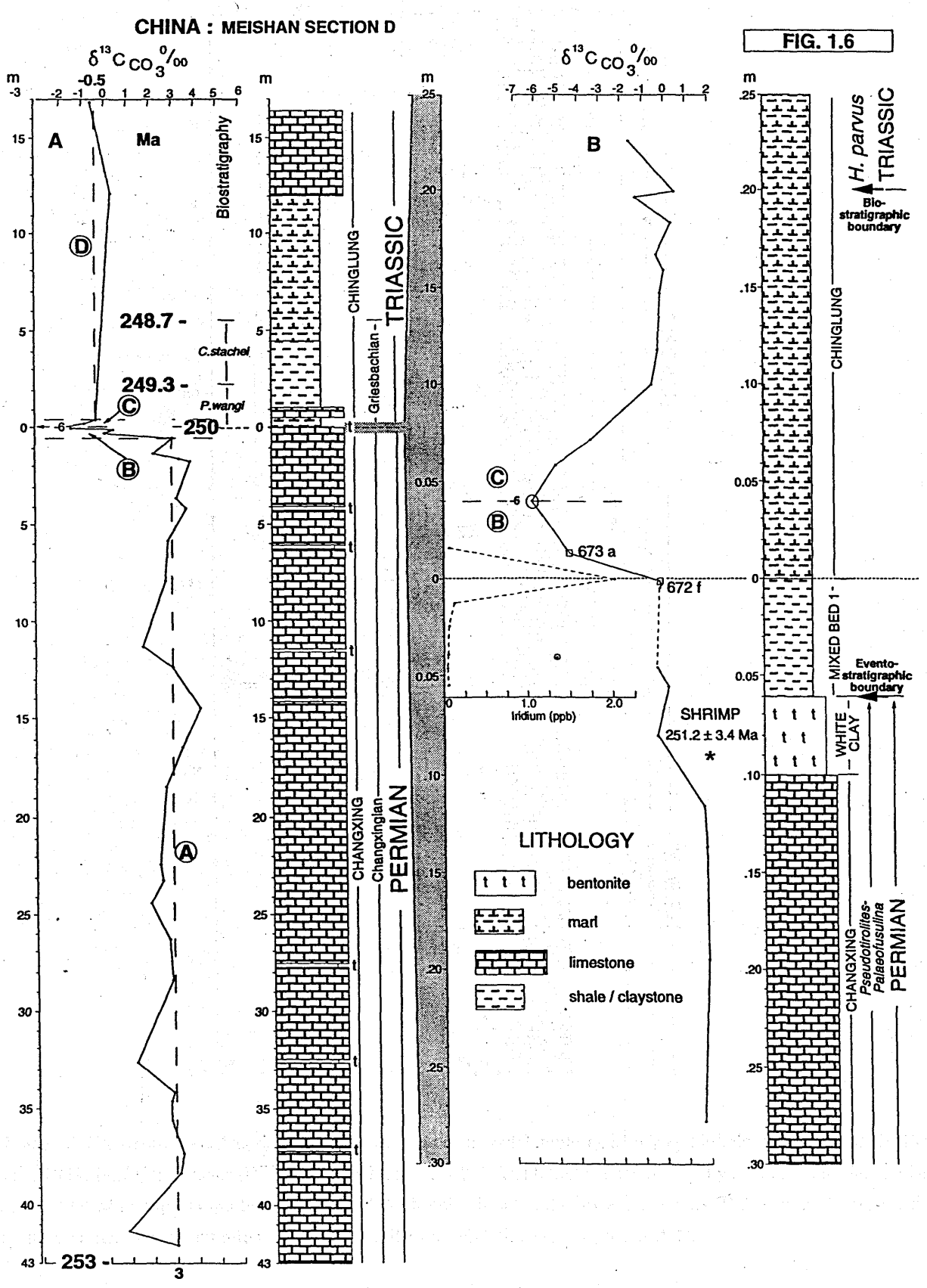
CHINA : MEISHAN SECTION D
FIG. 1.6
δ13C CO3 0/00
A
Ma
Biostratigraphy
D
C
B
A
248.7 -
C.stachei
249.3 -
P.wangi
250
253 -
CHINGLUNG
Griesbachian
TRIASSIC
CHANGXING
Changxinglan
PERMIAN
673 a
672 f
Iridium (ppb)
SHRIMP
251.2 ± 3.4 Ma
*
LITHOLOGY
bentonite
marl
limestone
shale / claystone
H. parvus
Bio-stratigraphic boundary
MIXED BED 1
Evento-stratigraphic boundary
WHITE CLAY
Pseudotirolites-Palaeofusulina

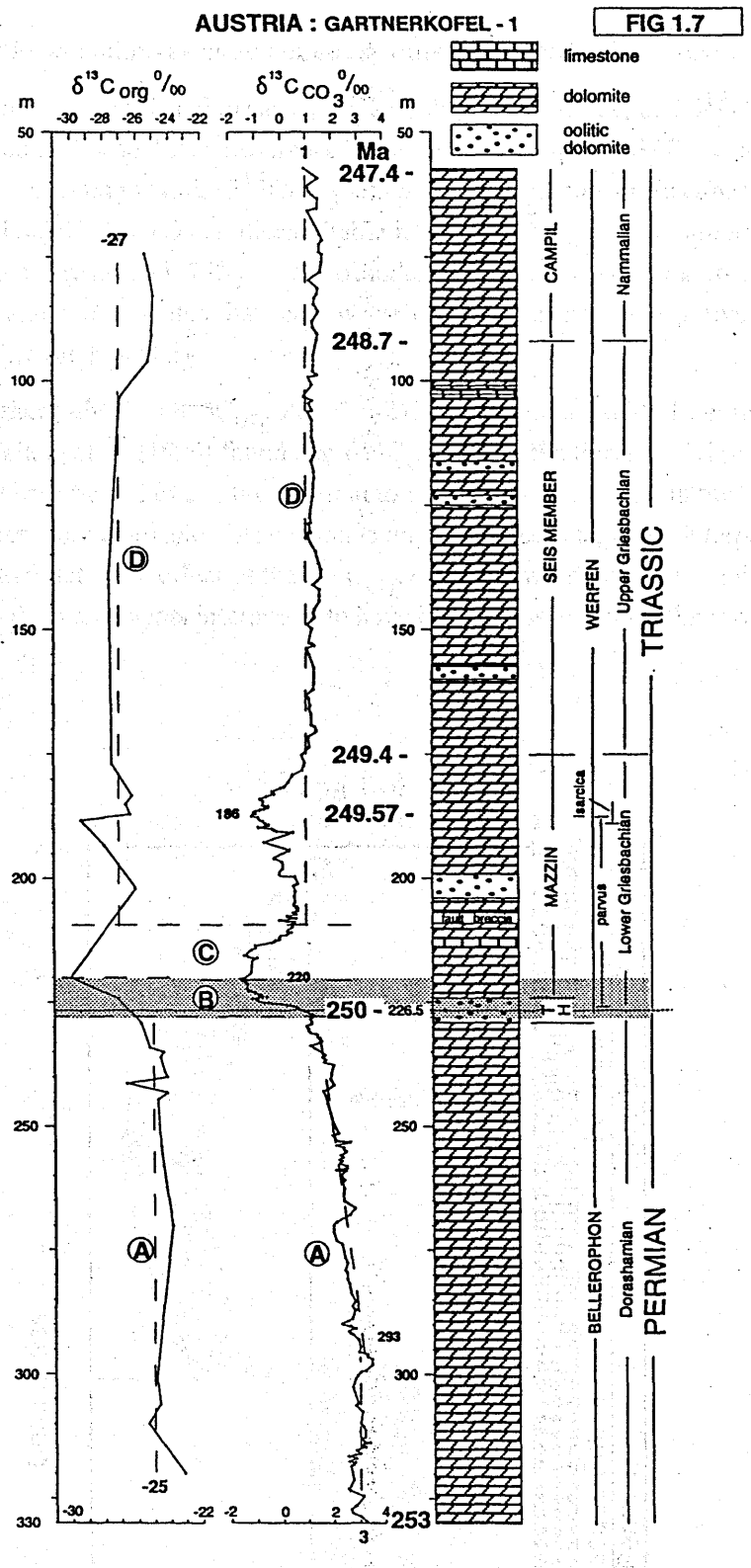

Figure 1.7 Gartnerkofel-1, Austria, $\delta^{13}C_{org}$ (Magaritz et al., 1992, table 1), $\delta^{13}C_{CO_3}$, lithology, formations (Holser et al., 1989, fig.2), and stages (Holser et al, 1991, p. 220-221). The timescale determined by assuming the Nammalian top at 247.4 Ma = top Campil Formation. The Griesbachian is split into Lower and Upper (Holser et al., 1991, p. 220, fig. 8) assumed of equal duration. The $\delta^{13}C$ profiles are subdivided into segments A-D.

1.6 $\delta^{13}C_{org}$ across the Permian-Triassic boundary outside of Australia - previous work

The Gartnerkofel-1 Core is unique as a parallel record of $\delta^{13}C_{CO3}$ and $\delta^{13}C_{org}$ across the Permian-Triassic boundary, with Δ (the difference between $\delta^{13}C_{CO3}$ and $\delta^{13}C_{org}$) around -27 ‰ throughout (Fig 1.7) suggesting that the $\delta^{13}C_{CO3}$ and $\delta^{13}C_{org}$ signatures reflect primary events despite the carbonate material having been dolomitised. Stable Permian $\delta^{13}C_{org}$ values are around -24‰, Early Triassic $\delta^{13}C_{org}$ values are around -27‰. The Gartnerkofel-1 study was the first to establish the validity of studying $\delta^{13}C_{org}$ and demonstrated that shallow shelf facies preserve the negative $\delta^{13}C_{org}$ excursion across the Permian-Triassic boundary.

In the only other published $\delta^{13}C_{org}$ Permian-Triassic boundary study from north British Columbia (Fig.1.8), Wang et al. (1994) found that $\delta^{13}C_{org}$ across the Permian-Triassic boundary shifted from values more positive than -30‰ in the Permian to values less than -30‰ in the Triassic in a 4 m interval. No carbonates were available. The section is important because, being interpreted as a deep water basinal facies, it demonstrates the effect of the $\delta^{13}C_{org}$ exursion in a deep water environment to complement the data from sediments interpreted to have been deposited in shallow water environments elsewhere.

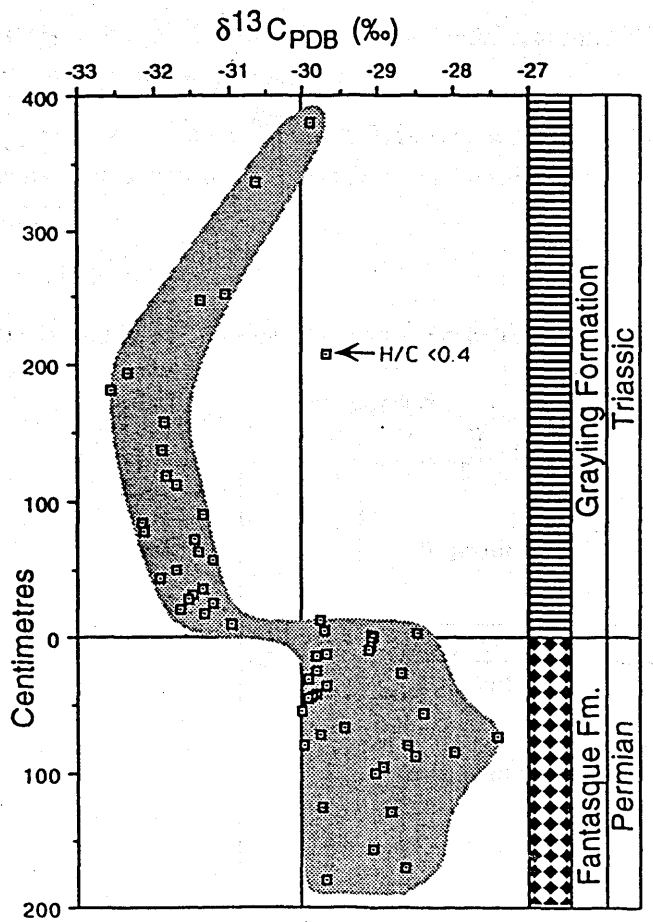

Figure 1.8 $\delta^{13}C_{org}$ profile from kerogens across the Permian-Triassic boundary at Williston Lake, British Columbia (from Wang et al., 1994).

1.7 The nonmarine $\delta^{13}C$ record - previous work

No $\delta^{13}C$ record in either carbonate or organic carbon across the nonmarine Permian-Triassic boundary existed before this study. However, Thackery et al. (1990) recorded a secular variation to more negative $\delta^{13}C$ values from tooth apatite of *Diictodon*, a mammal-like herbivorous reptile in the Lower Beaufort Formation of South Africa they interpreted as reflecting lower primary productivity and increased continental aridity toward the close of the Permian.

Correlation between marine and nonmarine environments of deposition using $\delta^{13}C$ chemostratigraphy was demonstrated for the Paleocene/Eocene boundary (Koch et al., 1992) where a $\delta^{13}C_{CO3}$ excursion was correlated between marine carbonate, paleosol carbonate, and mammalian tooth enamel. This is unusual because local environmental and diagenetic effects commonly overprint nonmarine primary $\delta^{13}C_{CO3}$ records but it encouraged the searching of Australian Permian-Triassic siliciclastics for evidence of the negative $\delta^{13}C$ excursion in nonmarine organic carbon.

1.8 Analysis of $\delta^{13}C$ profiles

The $\delta^{13}C_{CO3}$ profiles at the Permian-Triassic boundary may be divided into 4 clearly defined segments labelled **A-D** (Fig. 1.9). The segments represent:

- **A** a period of relatively stable $\delta^{13}C$ values in the Late Permian around 3‰ or higher in carbonate sections and -24.5‰ in organic carbon sections.
- **B** a period of falling $\delta^{13}C$ values about the Permian-Triassic boundary reaching a minimum in the Early Triassic in all sections except Meishan Section D (if the Permian-Triassic boundary is accepted to be midway through bed 27).
- **C** a positive excursion in $\delta^{13}C$.
- **D** a period of relatively stable $\delta^{13}C$ values during the Early Triassic that are more negative by 3 to 5‰ than those of segment A.

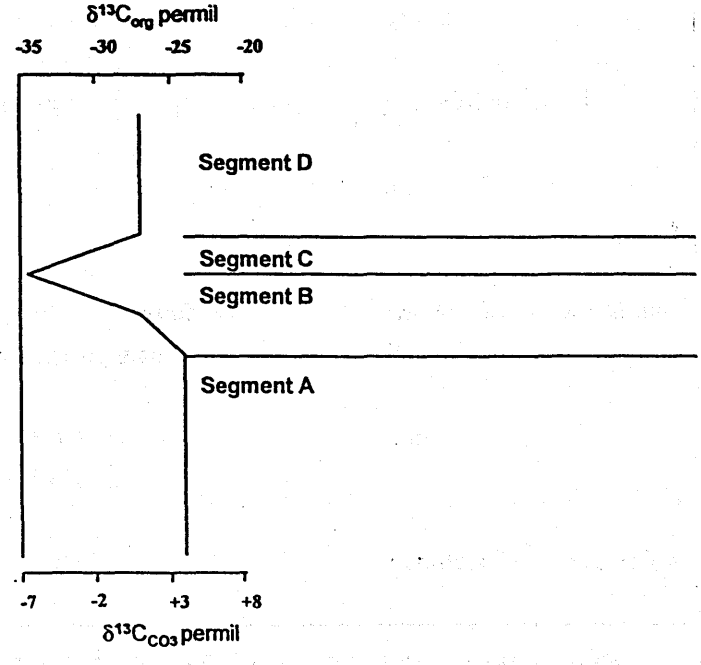

Figure 1.9 $\delta^{13}C$ profiles divided into segments A-D across the Permian-Triassic boundary.

1.9 $\delta^{13}C$ reference section

Newell (1994) regarded the $\delta^{13}C$ negative excursion as pivotal in defining the Permian-Triassic boundary. The negative $\delta^{13}C$ excursion is ubiquitous in carbonate sections about the paleontological Permian-Triassic boundary throughout Tethys (Baud et al, 1989; Holser et al, 1991), South China (Baud et al., 1989; Chen et al., 1991; Xu and Yan, 1993), and in Greenland (Oberhansli et al. 1989). The negative $\delta^{13}C$ excursion about the Permian-Triassic boundary therefore provides an isochronous datum for the determination of the Paleozoic/Mesozoic erathem boundary (Xu and Yan, 1993; Newell, 1994; Yin et al. 1994). To use such a correlation scheme, however, a reference section must be identified that satisfies the following criteria:

1. Detailed $\delta^{13}C$ analysis on stratigraphically controlled samples within the section available.

2. The terminal Permian and basal Triassic located by biostratigraphy.

3. The section should be complete.

Two candidate sections, Meishan Section D and the Gartnerkofel Core-1, are here chosen as reference sections for the reference isotope profile across the Permian-Triassic boundary. Neither is perfect and a discussion of each section's features follows.

	Meishan Section D	**Gartnerkofel Core-1**
Excursion magnitude	9‰	3.5‰
Excursion length in sediment column	< 1 m	> 10 m
$\delta^{13}C$ excursion organics/carbonates	carbonates only	carbonates and organic carbon
Evidence of alteration	unknown	yes - dolomitised
Evidence of an hiatus at the boundary	no	no
Biostratigraphical control	*Hindeodus parvus* above *H. changxingensis*	*Hindeodus parvus* above Paleofusulinids
Radiometric date	251.2 ± 3.4 Ma (SHRIMP)	none
$\delta^{18}O$ excursion	not reported	parallels $\delta^{13}C$ excursion

The $\delta^{13}C$ excursion occurs in < 1 m in Meishan Section D (Fig.1.6) and >10 m in the Gartnerkofel-1 Core section (Holser and Magaritz, 1992) (Fig. 1.7) indicating the Meishan Section D is condensed.

In the Meishan Section D, *H. parvus* (Permian-Triassic boundary index fossil) first occurs 8 cm above the base of bed 27 (= Bed 27C; Yin, 1993; Zhang, 1987). Bed 27 is the equivalent of the mixed bed 2 of Sheng (1984) and Xu and Yan (1993, fig. 1). Conodont fragments reminiscent of, but not positively identifed as *H. parvus* occur near the base of bed 27 (Yin, et al., 1994), hinting it is possible that the actual position of the Permian-Triassic boundary based on the first appearance of *H. parvus* may move down section to the base of Bed 27 from Bed 27C should a specimen of *H. parvus* be found lower in the section. The base of Bed 27 (top of mixed bed 1 of Sheng et al., 1984) in the Meishan Section D is therefore accepted as approximating the Permian-Triassic boundary (Fig. 1.6). Accordingly the most negative $\delta^{13}C_{CO3}$ value in the Meishan Section D profile lies in the earliest Triassic, not the latest Permian as would be the case with accepting the first appearance of *H. parvus* as the boundary (Xu and Yan, 1993). In other sections (Fig. 1.4), the most negative $\delta^{13}C$ value lies in the earliest Triassic so this placement would bring Meishan Section D in line with other Permian-Triassic boundary sections. The problem with accepting the first appearance of *H. parvus* as marking the biostratigraphic Permian-Triassic boundary is caused by the perceived need for a clear indicator fossil which makes its first appearance at the boundary. *H. parvus* appears 20cm above the eventostratigraphic horizon at the base of mixed bed 1, Meishan Section D where a Triassic-like fauna first appears but unfortunately the eventostratigraphic horizon is not clearly associated with an incoming conodont zone so is not "acceptable" as a biostratigraphic boundary (Wang, 1995). The biostratigraphic boundary as favoured by the PTWG (Bed 27C) is therefore not at the "event" associated with the extinctions at the Permian-Triassic boundary at Meishan Section D but is at a convenient biostratigraphic marker, namely the incoming of *H. parvus*.

The most "reliable" radiometric date of the Permian-Triassic boundary is from Meishan Section D (251.2±3.4 Ma) from zircons in the white clay analysed by the U/Pb method on the Sensitive High Resolution Ion Micro Probe or SHRIMP (Claoué-Long et al., 1991) (Fig. 1.6).

The Gartnerkofel Core-1 with more than 300 $\delta^{13}C$ analyses (Fig. 1.7), is the most detailed $\delta^{13}C$ study to date of any single section (Holser and Schönlaub, 1991). Biostratigraphical and lithological evidence indicates that it is also a complete sequence of the latest Permian and earliest Triassic. *H. parvus (Isarcicella? parva)*, in the top Tesero Horizon at the base of the Mazzin Member of the Werfen Formation (Holser et al., 1989) succeeds a fauna of diverse Permian taxa (Wignall and Hallam, 1992; Broglio Lorigo et al., 1986; Nerri et al., 1986; Noé, 1987); and sedimentological evidence indicates a gradational transition from the Bellerophon Formation into the Tesero Horizon (Wignall and Hallam, 1992). The carbon isotope profile gradually changes to more negative $\delta^{13}C_{CO3}$ values from around 3‰ within the Bellerophon Formation at 293 m to values of 1.5‰ at the Tesero Horizon at 231 m before rapidly becoming more negative at around -1.5% at 220 m within the basal Mazzin Member (Holser et al., 1989). Three $\delta^{13}C$ minima are found in Gartnerkofel-1. Two of these are above the paleontologically determined Permian-Triassic boundary at 193 and 186 m (Holser et al, 1989; 1991). The 186m minimum is not recognised in other published Permian-Triassic sections and may be, 1) unique in this section, 2) a reflection of local basinal conditions, or 3) an artifact of diagenesis.

The $\delta^{13}C_{org}$ profile of the Gartnerkofel Core section parallels the $\delta^{13}C_{CO3}$ profile (Magaritz et al. 1992). No secondary mechanism is known which shifts the $\delta^{13}C_{org}$ and $\delta^{13}C_{CO3}$ in parallel (Knoll et al., 1986), hence the isotopic excursion at the Permian-Triassic boundary in the Gartnerkofel Core-1 section is almost certainly a reflection of a primary event.

In summary, Meishan Section D has a sharp negative $\delta^{13}C_{CO3}$ excursion that could indicate a disconformity or an extremely condensed section (Baud et al., 1989), lacks a $\delta^{13}C_{org}$ profile but contains

the numerical calibration of the Permian-Triassic boundary (Claoué-Long et al., 1991). Gartnerkofel Core-1 has a parallel $\delta^{13}C_{org}$ and $\delta^{13}C_{CO3}$ profile but the profile is unique in terms of the number of negative excursions and much of the section has been dolomitised indicating possible isotopic re-equilibration.

Overall, the Gartnerkofel-1 section is probably the better reference section, with Meishan Section D a valuable support section.